GLOBAL SCIENCE LIBRARY

RESEARCH

Journal of Clinical & Medical Imaging

Use-fullness of dynamic contrast-enhanced MR imaging and diffusion weighted MR imaging for differentiation of benign and malignant parotid tumors

Zheng SY[1], Xu ZF[2*], Wu XH[1] and Pan AZ[2]

[1]Department of MR, Shantou Central Hospital, Shantou,Guangdong, China

[2]Department of Radiology, The First People's Hospital of Foshan, Guangdong, China

Abstract

Objectives: *To evaluate the usefullness of dynamic contrast-enhanced MR Imaging (DCE-MRI) and diffusion weighted imaging (DWI) for differentiating benign from malignant parotid tumors.*

Methods: *Prospectively,DCE-MRI and DWI were performed in 112 patients, with 148 confirmed parotid masses. The differential optimal thresholds were determined.*

Results: *WConsidering tumors with time-intensity curve (TIC) Type C as malignant, sensitivity, specificity, accuracy were 95%, 76%, 79%, respectively. Considering ADC threshold values $0.709\times10^{-3}mm^2/s<ADC<0.948\times10^{-3}mm^2/s$ as malignant, sensitivity, specificity, accuracy were 75%, 78%, 78%, respectively. Considering TIC Type C and ADC values $0.709\times10^{-3}mm^2/s<ADC<0.948\times10^{-3}mm^2/s$ as malignant, sensitivity, specificity, accuracy were 75%, 91%, 89%, respectively. With threshold $K_{ep}<1.118\ min^{-1}$ and $V_e>0.315$ between Warthin and malignant tumors, threshold $K_{ep}>0.555\ min^{-1}$ and $V_e<0.605$ between pleomorphic adenomas and malignant tumors, sensitivity, specificity, accuracy for malignancy were 70% vs 90%, 96% vs 74%, 92% vs 80%, respectively.*

Conclusion: *DCE-MRI and DWI provide more information in differentiating benign from malignant parotid tumors.*

Keywords: malignant parotid tumors, diffusion weighted imaging, MR imaging,optimal thresholds

Introduction

Nearly 80% of salivary gland tumors occur in the parotid glands [1]. Parotid gland tumors are very diverse in terms of histopathology and vicinity to facial nerves. The majority of these tumors are benign. However, sometimes they tend to transform into a malignant form; for example, nearly 20% of untreated pleomorphic adenomas could acquire malignancy [2]. On the other hand, a Warthin tumor shows less than 1% chance of malignant degeneration [3]. Therefore, pre-operative diagnosis and differentiation of benign and malignant tumors are a challenge for radiologists [2].

Owing to superb soft tissue resolution, MRI has a good ability to clearly identify the exact location and extent of a tumor, and differentiates histological characteristics such as mucin, fibrosis, chondromyxoid stroma, and hemorrhagic change within the tumor, which may provide some indication regarding its pathologic nature [4]. Although conventional MR imaging techniques have been used to diagnose salivary gland tumors, many investigators reported that differentiation of salivary gland tumors, especially benign and low-grade malignant tumors, is often difficult [4,5].

In recent years, functional MR imaging techniques such as dynamic contrast enhanced (DCE) MRI and diffusion-weighted imaging (DWI) have significantly contributed to the diagnosis of parotid tumors [3,6,7]. Semi-quantitative analysis of DCE-MRI is based on time-intensity curve (TIC). Previous studies showed that T peak correlates closely with microvessel count and wash out ratio (WR), and accurately reflects the cellularity-stromal grade.Yabuuchi et al. [6] categorized TIC into four types (A, persistent; B, washout; C, plateau; D, flat) and found that TIC types A, B and D suggesting benignancy and type C suggesting malignancy exhibited high sensitivity but relatively low specificity. DWI analysis is performed according to water molecule diffusion in a tissue for determining the cellularity of tumors [5,7]. Recent studies found that the combined use of DCE-MRI and DWI can greatly improve the diagnostic efficacy of MRI in differentiating benign and malignant salivary gland tumors [3,8]. Quantitative analysis of DCE-MRI is based on K_{trans}, K_{ep}, and V_e. This method has the potential to detect tumor angiogenesis. To our knowledge, the value of quantitative DCE-MRI in parotid tumor diagnosis has not been emphasized previously. The main objective of this study was to explore semi-quantitative and quantitative DCE-MRI with DWI for differentiation of benign and malignant parotid tumors.

Materials and Methods

Patients

This prospective study was approved by the institutional review board, and carried out between August 2013 and March 2016. DCE-MRI and DWI were prospectively performed on consecutive patients clinically suspected with primary parotid tumors in local hospital. Exclusion criteria were: hemangioma, lymphangioma, lipomyoma, cyst, which are easily diagnosis by clinical and radiological methods. All patients underwent surgery, and histopathologic diagnosis was based on findings in specimens obtained by surgical resection. Finally, 112 patients with 148 parotid masses confirmed by surgical pathology were included.

MR imaging protocol

MR imaging was performed on a 3.0T superconducting MR imaging system (Siemens MAGNETOM Verio 3.0T, Germany) with head and neck array coils. Routine MR sequence included tra-T1W(TR/TE, 550 ms/8.7 ms), tra-T2W (TR/TE, 5500 ms/95 ms)and cor-T2W-tirm (TR/TE/TI, 3000 ms/39 ms/220 ms). DCE–MRI was performed with a T1-weighted 3D spoiled gradient echo sequence (3D volume interpolated body examination, 3D-vibe; TR/TE, 5.08 ms/1.74 ms;flip angle 15°). The contrast agent Gd-DTPA (Magnevist, Schering, China) was injected after fourth dynamic sequence acquisition, at a rate of 2.0 ml/s, via the right antecubital vein. The contrast agent was administered at a concentration of 0.2 mmol/kg body weight. After contrast agent injection, a 20 mL saline flush at the same injection rate followed immediately. 35 dynamic sequence acquisitions, with 20 dynamic images per sequence, were carried out in a total scan time of 5 min 20s. Prior to dynamic image acquisitions, pre-contrast images were obtained with two flip angles of 2° and 15° for T1 mapping. DWI was performed with a multi-section spin-echo single-shot echoplanar sequence in the transverse plane with b values of 0, 500, and 1000s/mm^2, respectively. ADC maps were generated.

MR Image evaluation

An author, with more than 10 years of experience in head and neck MR diagnosis, who was blinded to histopathological results, manually drew regions of interests (ROIs) for each lesion. ROIs were drawn to avoid the vascular and cystic parts of the tumors. When contrast enhancement was heterogeneous, the signal intensities of multiple areas were measured, and the area with maximal enhancement was selected; the corresponding ROIs for ADC measurements were drawn. Semi-quantitative analysis of DCE-MRI was based on TIC. The latter was categorized into four types according to Yabuuchi' proposition [6]: Type A (persistent), increasing curve, time to peak more than 120 seconds; Type B (washout), rapidly increased washout phase, time to peak ≤120 seconds, with high washout ratio (≥30%); Type C (plateau), initial increase and slow washed out, time to peak ≤120 seconds, with low washout ratio (<30%); Type D, flat. Quantitative analysis of DCE-MRIwas based on the Tofts generalized mode [9]. In this model, the contrast agent movement between tissue compartments is related to three physiologically based parameters: K_{trans} (volume transfer constant between blood plasma and extracellular extravascular space [EES]), V_e (EES fractional volume) and K_{ep} (flux rate constant between the EES and plasma) [10].

Statistical analysis

All statistical analyses were performed with the Statistical Package for Social Sciences, Version 17.0 (SPSS 17.0). For comparison of TIC types in different histological types of parotid gland tumors, Pearson X^2 was used. ADC values, DCE-MRI quantitative parameters (K_{trans}, K_{ep}, and V_e,) among different histologic types of parotid gland tumors were assessed by the Kruskal-Wallis H test and Mann-Whitney U test. $P<0.05$ was considered statistically significant. Threshold values for various parameters were determined by receiver operating characteristic curve (ROC) based test. Sensitivity, specificity, accuracy, positive and negative predictive values for DWI and DCE-MRI in diagnosing malignant parotid tumors were calculated.

Results

Clinical and histopathologic results

Of the 112 cases, histopathology revealed 31 with pleomorphic adenoma (10 males and 21 females; age, 16-77 years, averaging 41 years), 52 with Warthin tumors (50 males and 2 females; age, 18-82 years, averaging 60 years; 18 cases with multiple lesions, for a total of 88 lesions), 20 with malignant tumors (9 males and 11 females; age, 22-68 years, averaging 52 years), and 9 with other benign tumors (basal cell adenoma, 5 cases; oncocytic adenoma, 1 case; monomorphic adenoma, 2 cases; facial nerve schwannoma, 1 case; 3 male and 6 females; age, 40-69 years, averaging 51 years).

Histopathologic diagnosis/TIC pattern		A	B	C	D
Benign	(n=128)	29	68	31	0
	Pleomorphic adenoma	27	0	4	0
	Warthin tumor	0	65	23	0
	basal cell adenoma	1	2	2	0
	Oncocytic adenoma	0	1	0	0
	Monomorphic adenoma	0	0	2	0
	Facial nerve schwannoma	1	0	0	0
malignant	(n=20)	0	1	19	0
	Squamous cell carcinoma	0	0	7	0
	Acinic cell carcinoma	0	1	2	0
	Lymphoepithelial carcinoma	0	0	3	0
	Adenoid cystic carcinoma	0	0	2	0
	lymphoma	0	0	1	0
	Mucoepidermoid carcinoma	0	0	1	0
	Duct carcinoma	0	0	1	0
	Basal cell adenocarcinoma	0	0	1	0
	Polymorphous low-grade adenocarcinoma	0	0	1	0

Table 1. *TIC Patterns among histopathologic diagnoses.*

TIC types among histopathologic diagnoses and diagnostic values

TIC types among histopathologic diagnoses are shown in Table 1. No tumor showed TIC D type in this study. 87% (27/31) pleomorphic adenoma showed TIC type A and 13% (4/31) had TIC type C; 74% (65/88) Warthin tumors showed TIC type B and 26% (23/88) had TIC type C. 95% (19/20) malignant tumors showed TIC type C, while 5% (1/20) were TIC type B. Pearson X2 test showed a significant difference between benign and malignant tumors in TIC patterns ($X^2=38.78$, $P<0.001$). We considered type A, B, and D TIC tumors as benign neoplasms, and type C TIC tumors

as malignant ones [3]. Sensitivity, specificity, accuracy, positive and negative predictive values were 95% (19/20), 76% (97/128), 79% (117/148), 38% (19/50), and 99% (97/98), respectively, when malignancy was considered a positive result.

ADC Cutoff levels and diagnostic values

ADC values for pleomorphic adenomas, Warthin tumors, and malignant tumors are shown in Table 2 and Figure 1. Kruskal-Wallis H test showed significant differences among the four groups (P<0.001). ADC values for pleomorphic adenomas were higher than those of malignant tumors, whereas ADC values for Warthin tumors were lower than those of malignant tumors. Thus, ADC thresholds were used to differentiate pleomorphic adenomas from malignant tumors, and Warthin tumors from malignant tumors by ROC based tests (Figures 2 and 3).

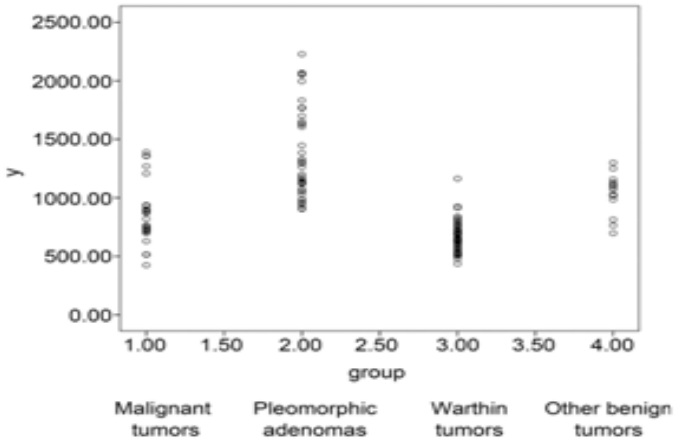

Figure 1. *Scatter plot showing the distribution of ADC values among various histologic tumors. Figure 2. ROC between pleomorphic adenomas and malignant tumors. The area under the curve (AUC) is 0.890.*

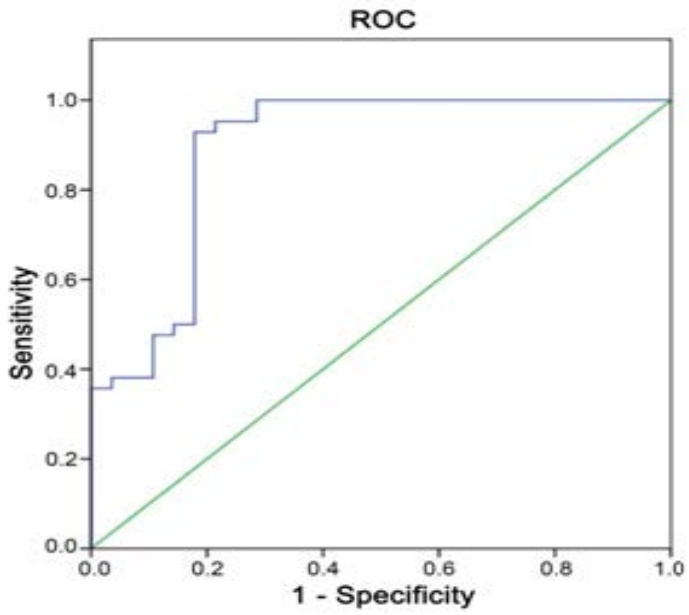

Figure 2. *ROC between pleomorphic adenomas and malignant tumors. The area under the curve (AUC) is 0.890.*

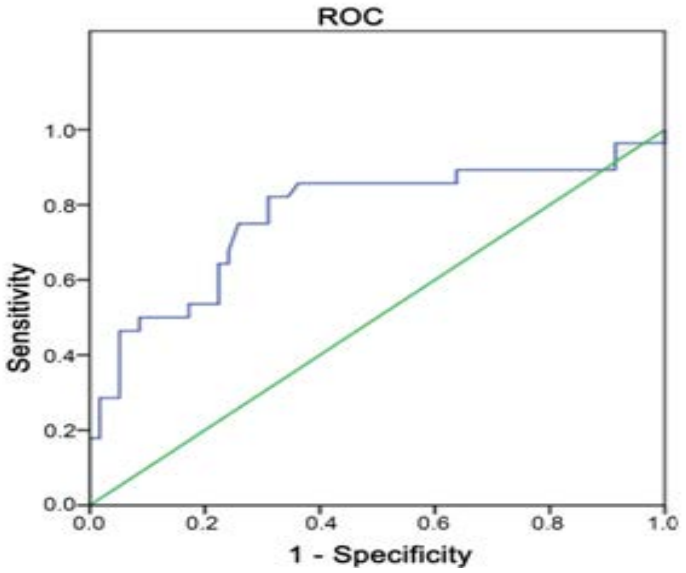

Figure 3. *ROC between Warthin tumors and malignant tumors. The area under the curve (AUC) is 0.771.*

	Min(×10-3mm²/s)	Max(×10-3mm²/s)	Mean(×10-3mm²/s)	Standard Deviation
Malignant tumors	0.424	1.39	0.858	0.253
Warthin tumors	0.436	1.164	0.669	0.126
Pleomorphic adenomas	0.904	2.228	1.367	0.376
Other benign tumors	0.698	1.3	1.036	0.168

Table 2. *ADC values among histopathologic diagnoses.*

ADC thresholds were $0.948\times10^{-3}mm^2/s$ between pleomorphic adenomas and malignant tumors, $0.709\times10^{-3}mm^2/s$ between Warthin tumors and malignant tumors; sensitivity values were 93% and 82%, respectively, with specificity values of 82% and 69%, respectively, for diagnosing malignant tumors. Considering ADC value of $0.709\times10^{-3}mm^2/s<ADC<0.948\times10^{-3}mm^2/s$ to reflect malignant tumors, sensitivity, specificity, accuracy, positive and negative predictive values were 75% (15/20), 78% (100/128), 78% (115/148), 35% (15/43), and 95% (100/105), respectively.

Diagnostic value DWI combined with TIC

Considering the TIC C pattern and ADC value $0.709\times10^{-3}mm^2/s$ $<ADC<0.948\times10^{-3}mm^2/s$ to reflect malignant tumors, sensitivity, specificity, accuracy, positive and negative predictive values were 75% (15/20), 91% (117/128), 89% (132/148), 58% (15/26) and 96% (117/122), respectively.

Quantitative DCE-MRI parameters in histopathologic diagnoses and their diagnostic values

Mean quantitative parameter values (Ktrans, Kep and Ve) among histopathologic diagnoses are shown in Tables 3 and 4.

ROC based tests showed cut-off $K_{trans}<0.435\ min^{-1}$, $K_{ep}<1.118\ min^{-1}$, and $V_e>0.315$ for differentiating malignant from Warthin

tumors, and sensitivity, specificity, accuracy, positive and negative predictive values were 70% (14/20), 96% (85/88), 92% (99/108), 82% (14/17), and 93% (85/91), respectively.

ROC based tests showed cut-off K_{ep}>0.555 min^{-1} and V_e<0.605 for differentiating malignant tumors from pleomorphic adenomas, and sensitivity, specificity, accuracy, positive and negative predictive values were 90% (18/20), 74% (23/31), 80% (41/51), 69% (18/26), and 92% (23/25), respectively.

Diagnostic values of the different diagnosis methods are shown in Table 5.

	K_{trans}(min^{-1})	K_{ep}(min^{-1})	V_e
Malignant tumors	0.327±0.030	0.784±0.064	0.445±0.025
Pleomorphic adenomas	0.217±0.036	0.567±0.048	0.549±0.278
Warthin tumors	0.464±0.036	1.806±0.111	0.272±0.013
Other benign tumors	0.663±0.092	1.358±0.205	0.528±0.431
Chi-square	22.062	76.552	78.685
P	0.035	0	0

Table 3. *Quantitative DCE-MRI parameters among histopathologic diagnoses.*

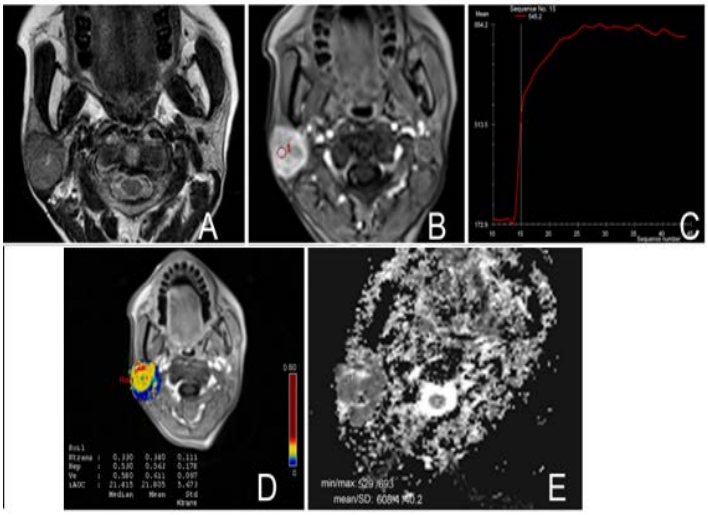

Figure 4. *Lymphoepithelial carcinoma. (A) Axial T2WI showing isodense nodules in the right parotid. (B) CE-T1WI showing non homogeneously enhanced nodule. (C) TIC of Pattern C. (D) Ktrans graph showing Ktransvalue of 0.340 min^{-1}, Kepvalue of 0.563 min^{-1}, and V_e of 0.611; (E) ADC value is 0.608×$10^{-3}$$mm^2$/s.*

		K_{trans}(min^{-1})	K_{ep}(min^{-1})	V_e
malignant tumors and pleomorphic adenomas	*Z*	*-1.328*	*-2.866*	*-2.243*
	P	*0.184*	*0.004*	*0.025*
malignant tumors and Warthin tumors	*Z*	*-2.069*	*-5.706*	*-5.497*
	P	*0.039*	*0*	*0*

Table 4. *Quantitative DCE-MRI parameters among histopathologic diagnoses.*

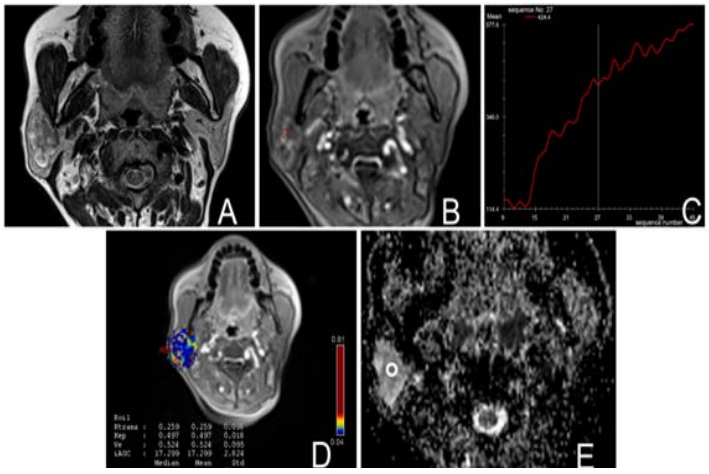

Figure 5. *Pleomorphic adenoma. (A) Axial T2WI showing a mixed hyper-dense and isodense nodules in the right parotid. (B) CE-T1WI showing non-homogeneous enhanced nodules. (C) TIC of Pattern A. (D) K_{trans} map showing K_{trans} value of 0.259 min^{-1}, K_{ep}value of 0.497 min^{-1}, and V_e of 0.524; (E) ADC value is 1.124×$10^{-3}$$mm^2$/s.*

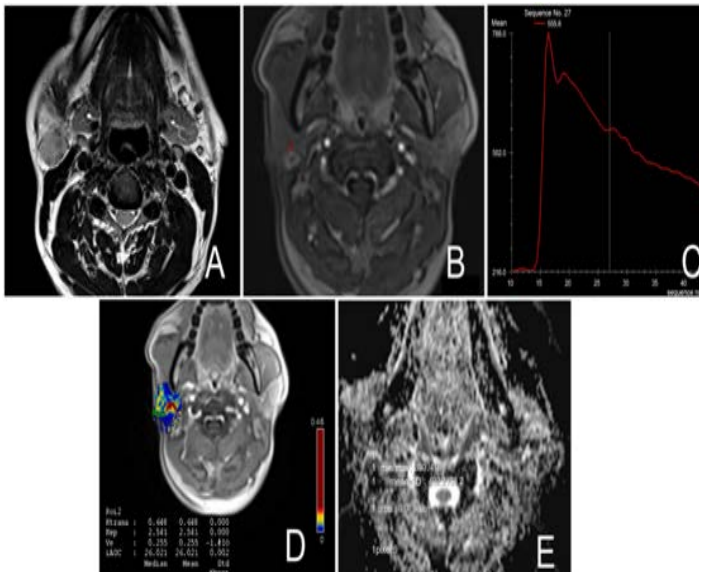

Figure 6. *Warthin tumor.(A) Axial T2WI showing hypodense nodules in the right parotid. (B) CE-T1WI showing a homogeneous enhanced nodule. (C) TIC of Pattern B. (D) Ktrans graph showing Ktransvalue of 0.648 min^{-1}, K_{ep} value of 2.541 min^{-1}, and V_e of 0.255; (E) ADC value is 0.402×$10^{-3}$$mm^2$/s.*

MRI, DCE-MRI, TIC, Ktrans graphs and ADC maps of malignant tumor, pleomorphic adenomas and Warthin were showed on Figures 4 to 6.

Discussion

Previous reports [6,11], revealed close associations of TTP with microvessel count and angiogenesis, while WR also showed a close relationship with cellularity. A large extracellular space with fibrous stromata retains contrast material for a certain period; therefore, tumors with high cellularity-stromal grade will retain less contrast material and have a high WR.

Diagnosing malignant tumors Table 5. Diagnostic value of different diagnosis methods. (%)					
Methods/diagnostic value	**Sensitivity**	**Specificity**	**Accuracy**	**Positive predictive values**	**Negative predictive values**
TIC	95	76	79	38	99
ADC	75	78	78	35	95
ADC combined TIC	75	91	89	58	96
Quantitative analysis between malignant tumors and Warthin tumors	70	96	92	82	93
Quantitative analysis between malignant tumors and pleomorphic adenomas	90	74	80	69	92

Table 5. Diagnostic value of different diagnosis methods.

In this study, 95% of malignant parotid tumors showed a plateau TIC pattern due to high microvessel count and low cellularity-stromal grade; however, one acinic cell carcinoma (5%) had a different TIC pattern (washout pattern) because of its high cellularity in histologic analysis, corroborating findings by Yabuuchi et al. [3] 75% of Warthin tumors had a washout TIC pattern, which could be explained by their high microvessel count and high cellularity-stromal grade. While 26% had a plateau TIC pattern, pathological analyses showed inflammatory reactions in the tumors, which may decrease the cellularity-stromal grade and help retain contrast material for a certain period. 87% pleomorphic adenomas had a persistent TIC pattern; this could be explained by that microscopically pleomorphic adenoma shows a mixture of epithelial tissue intermingled with myxoid, mucoid or chondroid areas. Such tumors have a low microvessel count and reduced cellularity-stromal grade, and therefore have a long TTP [4]. However, there were four pleomorphic adenomas (13%) with a plateau TIC pattern. Pathology showed these tumors were rich in epithelial tissue, with high microvessel counts and low cellularity-stromal grade; they were hard to differentiate from malignant tumors by TIC, in agreement with Yabuuchi et al. [6] and Takashima et al. [11]. Considering type A, B, and D TIC tumors as benign neoplasms and type C as malignant, high sensitivity but relatively low specificity were obtained when malignancy was considered a positive result because of the inclusion of some benign tumors. In patients with plateau TIC pattern tumors, malignant tumors should be differentiated from pleomorphic adenomas and Warthin tumors. However, pleomorphic adenomas do not have to be differentiated from Warthin tumors in patients with washout and persistent pattern tumors, because Warthin tumors never show a persistent TIC pattern, and conversely, pleomorphic adenomas do not have a washout TIC pattern.

In this study, mean ADC value for pleomorphic adenoma was highest [$(1.367\pm0.376)\times10^{-3}mm^2/s$], followed by malignant tumors [$(0.859\pm0.254)\times10^{-3}mm^2/s$]; the lowest was Warthin tumors [$(0.700\pm0.126)\times10^{-3}mm^2/s$). Of note, there was an overlap between benign and malignant tumors. Our results were similar to previously reported findings. For example, Ikeda et al. [12] showed that ADCs of Warthin tumors are significantly lower than those of malignant tumors. The same study group demonstrated that cellularity of tumors affects their ADC levels [7,13,14]. Motoori et al .[15] revealed the significance of myxomatous tissue detection on MR images in differentiating pleomorphic adenomas from malignant tumors. Eida et al. [5] found that myxomatous tissues have high ADCs. Thus, ADC Maps show that more frequently, areas with a high ADC value ($>1.8\times10^{-3}mm^2/s$) have significantly more benign than malignant parotid tumors. Unlike this study, Eida et al proposed criteria based on ADC levels by dividing the calculated values in 4 groups (extremely low, low, intermediate, and high), with ADC levels calculated from different areas of each tumor. In the present study, ADC values were measured on areas corresponding to maximal enhancement on DCE-MRI. Using ADC values, we correctly modified the diagnosis of four epithelial-dominant pleomorphic adenomas that showed a plateau TIC pattern because of their high ADC values. Specificity, accuracy, and positive predictive values were improved with addition of DWI to DCE-MRI TIC.

DCE-MRI can be used to measure tissue perfusion by fast repeated scans of the same tissue volume before administration of gadolinium and during its passage through the tissue [16]. In this study, we found Warthin tumors had the highest Ktrans, followed by malignant tumors, and pleomorphic adenomas. This is due to tumor vessel counts, which were related to TTP in TIC. Pleomorphic adenomas had the highest Ve, followed by malignant tumors, and Warthin tumors, which is attributed to tumor extracellular extravascular space, in turn related to WR in TIC. Compared with TIC, DCE-MRI quantitative parameters have the advantages of better quantification of vessel permeability, with more quantitative data [17-19]. In the current study, with $K_{trans}<0.435\ min^{-1}$, $K_{ep}<1.118\ min^{-1}$, and $V_e>0.315$ as cutoff values for differentiating malignant from Warthin tumors, and $K_{ep}>0.555\ min^{-1}$ and $V_e<0.605$ for differentiating malignant tumors from pleomorphic adenomas, the diagnosis value was improved compared with that of TIC.

However, some limitations of this study should be mentioned. There were a small number of malignant tumors, and we did not classify them by pathological pattern.

Discussion

In conclusion, semi-quantitative and quantitative analysis of DCE-MRI in combination with DWI could provide more information, with added value in the differentiation of benign and malignant parotid tumors.

References

1. Speight PM, Barrett AW. Salivary gland tumours. *Oral Dis.* 2002;8:229-240.
2. Assili S, FathiKazerooni A, Aghaghazvini L, Saligheh Rad HR, Pirayesh Islamian J. Dynamic Contrast Magnetic Resonance Imaging (DCE-MRI) and Diffusion Weighted MR Imaging (DWI) for Differentiation between Benign and Malignant Salivary Gland Tumors. *J Biomed Phys Eng.* 2015;5:157-168.
3. Yabuuchi H, Matsuo Y, Kamitani T, Setoguchi T, Okafuji T, et al. Parotid gland tumors: can addition of diffusion-weighted MR imaging to dynamic contrast-enhanced MR imaging improve diagnostic accuracy in characterization? *Radiology.* 2008;249:909-916.
4. Okahara M, Kiyosue H, Hori Y, Matsumoto A, Mori H, et al. Parotid tumors: MR imaging with pathological correlation. *Eur Radiol.* 2003;13:L25-L33.
5. Eida S, Sumi M, Sakihama N, Takahashi H, Nakamura T. Apparent diffusion coefficient mapping of salivary gland tumors: prediction of the benignancy and malignancy. *AJNR Am J Neuroradiol.* 2007;28:116-121.
6. Yabuuchi H, Fukuya T, Tajima T, Hachitanda Y, Tomita K, et al. Salivary gland tumors: diagnostic value of gadolinium-enhanced dynamic MR imaging with histopathologic correlation. *Radiology.* 2003;226:345-354.
7. Habermann CR, Arndt C, Graessner J, Diestel L, Petersen KU, et al. Diffusion-weighted echo-planar MR imaging of primary parotid gland tumors: is a prediction of different histologic subtypes possible? *AJNR Am J Neuroradiol.* 2009;30:591-596.
8. Eida S, Sumi M, Nakamura T. Multiparametric magnetic resonance imaging for the differentiation between benign and malignant salivary gland tumors. *J Magn Reson Imaging.* 2010;31:673-679.
9. Tofts PS, Brix G, Buckley DL, Evelhoch JL, Henderson E, et al. Estimating kinetic parameters from dynamic contrast-enhanced T(1)-weighted MRI of a diffusable tracer: standardized quantities and symbols. *J Magn Reson Imaging.* 1999;10:223-232.
10. Jackson AS, Reinsberg SA, Sohaib SA, Charles-Edwards EM, Jhavar S, et al. Dynamic contrast-enhanced MRI for prostate cancer localization. *Br J Radiol.* 2009;82:148-156.
11. Takashima S, Noguchi Y, Okumura T, Aruga H, Kobayashi T. Dynamic MR imaging in the head and neck. *Radiology*. 1993;189:813-821.
12. Ikeda M, Motoori K, Hanazawa T, Nagai Y, Yamamoto S, et al. Warthin tumor of the parotid gland: diagnostic value of MR imaging with histopathologic correlation. *AJNR Am J Neuroradiol.* 2004;25:1256-1262.
13. Motoori K, Yamamoto S, Ueda T, Nakano K, Muto T, et al. Inter- and intratumoral variability in magnetic resonance imaging of pleomorphic adenoma: an attempt to interpret the variable magnetic resonance findings. *J Comput Assist Tomogr.* 2004;28:233-246.
14. Habermann CR, Gossrau P, Graessner J, Arndt C, Cramer MC, et al. Diffusion-weighted echo-planar MRI: a valuable tool for differentiating primary parotid gland tumors? *Rofo.* 2005;177:940-945.
15. Motoori K, Iida Y, Nagai Y, Yamamoto S, Ueda T, et al. MR imaging of salivary duct carcinoma. *AJNR Am J Neuroradiol.* 2005;26:1201-1206.
16. Viallon M, Cuvinciuc V, Delattre B, Merlini L, Barnaure-Nachbar I, et al. State-of-the-art MRI techniques in neuroradiology: principles, pitfalls, and clinical applications. *Neuroradiology.* 2015;57:441-467.
17. Yeo DM, Oh SN, Jung CK, Lee MA, Oh ST, et al. Correlation of dynamic contrast-enhanced MRI perfusion parameters with angiogenesis and biologic aggressiveness of rectal cancer: Preliminary results. *J Magn Reson Imaging.* 2015;41:474-480.
18. Chung WJ, Kim HS, Kim N, Choi CG, Kim SJ. Recurrent glioblastoma: optimum area under the curve method derived from dynamic contrast-enhanced T1-weighted perfusion MR imaging. *Radiology.* 2013;269:561-568.
19. Thomas AA, Arevalo-Perez J, Kaley T, Lyo J, Peck KK, et al. Dynamic contrast enhanced T1 MRI perfusion differentiates pseudoprogression from recurrent glioblastoma. *J Neurooncol.* 2015;125:183-190.

Correspondence: Xu ZF, Department of Radiology, The First People's Hospital of Foshan, Guangdong, China, Tel: +86 757 2233 3098; E-mail: xuzf83@126.com

Received: May. 10, 2018; Accepted: May 23, 2018; Published: May 28, 2018

J Clin Med Imag. 2018;1(1):1
DOI: gsl.jcmi. 2018.00001